

AMERICAN UNIVERSITY OF BEIRUT

SEISMIC STRENGTHENING OF BOND-CRITICAL
REGIONS IN WALL-TYPE BRIDGE PIERS USING ACTIVE
CONFINEMENT

by
FARIS ANWAR HADDADIN

A thesis
submitted in partial fulfillment of the requirements
for the degree of Master of Engineering
to the Department of Civil Engineering
of the Faculty of Engineering and Architecture
at the American University of Beirut

Beirut, Lebanon
December 2014

AMERICAN UNIVERSITY OF BEIRUT

SEISMIC STRENGTHENING OF BOND-CRITICAL
REGIONS IN WALL-TYPE BRIDGE PIERS USING ACTIVE
CONFINEMENT

by
FARIS HADDADIN

Approved by:

Dr. ElieHantouche, Assistant Professor
Civil and Environmental Engineering



Advisor

Dr. Mohamed Harajli, Professor
Civil and Environmental Engineering



Co-Advisor

Dr. Ghassan Chehab, Associate Professor
Civil and Environmental Engineering



Member of Committee

Date of thesis defense: November 28, 2014

AMERICAN UNIVERSITY OF BEIRUT

THESIS, DISSERTATION, PROJECT RELEASE FORM

Student Name: Haddadin, Faris Anwar
Last First Middle

Master's Thesis Master's Project Doctoral Dissertation

I authorize the American University of Beirut to: (a) reproduce hard or electronic copies of my thesis, dissertation, or project; (b) include such copies in the archives and digital repositories of the University; and (c) make freely available such copies to third parties for research or educational purposes.

I authorize the American University of Beirut, **three years after the date of submitting my thesis, dissertation, or project**, to: (a) reproduce hard or electronic copies of it; (b) include such copies in the archives and digital repositories of the University; and (c) make freely available such copies to third parties for research or educational purposes.

J. Haddadin
Signature

13 January 2015
Date

ACKNOWLEDGEMENTS

The author wishes to extend his sincere appreciation to Dr. Mohamed Harajli for giving him an opportunity to work on this thesis and for providing him support. The author would like to express his profound gratitude to Dr. Elie Hantouche for his assistance and excellent guidance throughout the course of this research. The author is also very grateful to Dr. Ghassan Chehab, for his acceptance to participate in the graduate committee and his approval of this thesis. Without their invaluable advice, patience and feedback this work would not have been possible.

The author also wishes to thank all the faculty members of the Department of Civil Engineering of the Faculty of Engineering and Architecture at the American University of Beirut, for granting him the adequate education and knowledge to help during the academic years.

The author takes the opportunity to express his deep indebtedness to his role model and life-time mentor, his father, Anwar S. Haddadin.

Finally, the author wishes to thank his wife, family, and friends for their motivation, encouragement, and endless faith.

AN ABSTRACT OF THE THESIS OF

Faris Anwar Haddadin for Master of Engineering
Major: Civil Engineering

Title: Seismic Strengthening of Bond-Critical Regions in Wall-Type Bridge Piers Using Active Confinement

Active confinement by means of pre-tensioned steel anchor rods was used in this investigation for bond strengthening of lap spliced reinforcement and for improving the seismic performance of wall-type bridge piers. As-built and strengthened representative pier specimens with lap spliced reinforcement within the critical hinging region were tested under large drift reversals. The test parameters included pier longitudinal reinforcement ratio, diameter of the spliced bars, and configuration of the pre-tensioned steel anchor rods. The strengthened columns developed enhanced bond resistance and low bond degradation of the spliced bars, increases in the lateral load and drift capacities, and much less pinching in the lateral load-drift response when compared with the as-built specimens. A design approach is proposed for evaluating the active lateral pressure required for adequate bond strengthening.

CONTENTS

	Page
ACKNOWLEDGEMENTS	v
ABSTRACT	vi
ILLUSTRATIONS	ix
TABLES	ixi
ABBREVIATIONS	ixii
Chapter	
1. INTRODUCTION AND LITERATURE REVIEW	1
1.1 Introduction	1
1.2 Review of Bond	3
1.3 Mechanism of Passive and Active Confinement	5
2. OBJECTIVE	7
3. EXPERIMENTAL PROGRAM	9
3.1 Test Specimens	9
3.2 Materials	15
3.2.1 Reinforcing Steel	15
3.2.2 Concrete	15
3.3 Construction of Specimens	16
3.3.1 Formwork	16
3.3.2 Fabrication of Cages	17
3.3.3 Casting	17

3.4 Loading Procedure and Instrumentation.....	19
4. DESIGN GUIDELINES.....	25
4.1 Guidelines.....	25
4.2 Design Example.....	30
4.3 Design Steps.....	31
5. TEST RESULTS AND ANALYSIS.....	34
5.1 General Behavior and Mode of Failure.....	35
5.2 Lateral load-drift Response.....	39
5.2.1 As-built Columns.....	39
5.2.2 Strengthened Columns.....	43
5.3 Energy Dissipation Capacities.....	44
6. CONCLUSIONS.....	46
 REFERENCES.....	 49

ILLUSTRATIONS

Figure	Page
Figure 1. Steel-concrete bond resistance components	4
Figure 2. Proposed strengthening system for wall-type bridge pier	11
Figure 3. Dimensions and reinforcement details of the column specimens.....	12
Figure 4. Lateral load applied at an effective height of 150 cm of the specimen.	14
Figure 5. Steel anchor rods and steel plates configuration.....	15
Figure 6. Side view of steel plates and anchor rods	16
Figure 7. Formwork with top wooden braces before and after casting.....	17
Figure 8. Formwork removed and specimen is erected	18
Figure 9. Specimen erected	19
Figure 10. Loading setup.....	20
Figure 11. Actual load testing carried out on specimen W20-SA.....	21
Figure 12. Maximum push cycle causing specimen W20-SA to tilt.....	21
Figure 13. Loading protocol.....	22
Figure 14. Steel plates configuration and wiring connections of the strain gauges for specimen W20-SA	25
Figure 15. Shear friction concept for evaluating the anchor pre-tension force.....	28
Figure 16. Concrete pressure distribution using active confinement	31
Figure 17. Crack path recording on W16-U specimen, during testing	35
Figure 18. Crack distribution in the as-built specimens of series W16.....	37
Figure 19. Crack distribution in the as-built specimens of series W20.....	37
Figure 20. Crack distribution in the as-built specimens of series W20.....	38
Figure 21. Crack distribution in the strengthened specimens of series W16	38

Figure 22. Crack distribution in the strengthened specimens of series W20	39
Figure 23. Crack distribution in the strengthened specimens of series W25	39
Figure 24. Lateral load-drift response for the as-built specimens in series W16	41
Figure 25. Lateral load-drift response for the strengthened specimens in series W16	41
Figure 26. Lateral load-drift response for the as-built specimens in series W20	42
Figure 27. Lateral load-drift response for the strengthened specimens in series W20	42
Figure 28. Lateral load-drift response for the as-built specimens in series W25	43
Figure 29. Lateral load-drift response for the strengthened specimens in series W25	43
Figure 30. Comparison of energy dissipation of as-built and strengthened specimens of series W20.....	45
Figure 31. Comparison of cumulative energy dissipation of as-built and strengthened specimens of series W20.....	46

TABLES

Table 1.	Specimens notations and strengthening techniques.....	13
Table 2.	Drift ratio, amplitude and its corresponding cycles.....	23
Table 3.	Relevant test parameters and results.....	34

ABBREVIATIONS

AASHTO	American Association of State Highway and Transportation Officials
ACI	American Concrete Institute
AISC	American Institute of Steel Construction
ANSI	American National Standards Institute
ASTM	American Society for Testing and Materials
CFRP	carbon fiber-reinforced polymer
cm	centimeter
d_b	bar diameter
f'_c	concrete compressive strength
FRP	fiber-reinforced polymer
kN	kilo Newton
ksi	kips per square inch
LRFD	load and resistance factor design
LVDT	linear variable differential transformer
m	meter
mm	millimeter
MPa	mega Pascale
RC	reinforced concrete

CHAPTER 1

INTRODUCTION AND LITERATURE REVIEW

1.1 Introduction

Lap splicing of longitudinal reinforcement at the base of columns in reinforced concrete (RC) building structures or piers in bridge structures has been a common practice in earlier years. While this practice leads to satisfactory performance in regions of low or no seismic hazard, it has a major drawback in areas of high seismic action. The fact that the splices are located within the critical hinging region of the column or pier, large drift and steel stress reversals induced by strong earthquakes cause bond splitting failure of the spliced bars and rapid bond and flexural strength degradation within the critical hinging region, leading to substandard seismic performance and possibly collapse of the structure. Field observations following major earthquakes clearly show that most structural damage or failure in bridges or buildings are attributed to inadequate detailing of lap spliced reinforcement (Mitchell, Sexsmith, and Tinawi 1994; Priestley, Seible, and Calvi 1996).

Several parameters influence the bond strength of developed or lap spliced steel bars in tension. Most important among them are the concrete cover, the development/splice length, the concrete compressive strength, and the area or amount of transverse steel confining reinforcement (Orangun, Jirsa, and Breen 1975; Darwin, Lutz, and Zuo 2005). For newly designed and constructed structures in regions of high seismic hazard, bond strength of steel bars in reinforced concrete members can be improved by providing adequate concrete cover, increasing the ratio of concrete cover

to bar diameter, and by using closely spaced transverse steel ties within the splice/development length; but most importantly by avoiding splicing of the reinforcement within the critical hinging regions. At present, in areas of high seismic hazard, the AASHTO LRFD (2011) prevents splicing of pier longitudinal reinforcement at the base of the pier.

For existing columns or bridge piers with bond-critical regions, the most conventional approach for improving the bond strength of developed or spliced steel bars in tension is by providing external confinement. In this context, a number of experimental studies have been carried out in recent years in which several external confinement techniques have been explored for seismic bond strengthening of reinforcing bars in circular and rectangular RC columns. Some of the techniques included the use of steel jackets (Mitchell et al. 1994; Priestly et al. 1996; Aboutaha, Engelhardt, Jirsa, and Kreger 1999), carbon fiber reinforced polymer (CFRP) jackets (Priestley et al. 1996; Seible, Priestly, Hegemier, and Innamorato 1997; Hawkins, Gamble, Shkurti, and Lin 2000; Harries, Ricles, Pessiki, and Sause 2006; Ghosh and Sheikh 2007; Harajli and Dagher 2008; Harajli and Khalil 2008; El Gawady, Endeshaw, McLean, and Sack 2010; Bournas, and Triantafillou, 2011; Hantouche and Harajli 2013), and most recently a combination of CFRP jackets and CFRP anchors (Kim, Jirsa, and Bayrak 2011). All of these studies reported enhanced bond performance of the reinforcement and improved seismic response of the columns.

The intent of the latter study (Kim, Jirsa, and Bayrak 2011) was to find an effective method of anchoring CFRP sheets to RC beams so that the ultimate tensile strength of the CFRP could be realized. CFRP sheets were anchored by a combination

of CFRP anchors and U-wraps. The specimens with anchorage showed some improvement in deformation capacity after peak load was reached. When CFRP anchors or CFRP U-wraps were used alone, delamination of the sheet led to failure of the anchor or U-wrap. Two main failure modes, failure of the CFRP sheets or failure of anchorage, were observed if additional anchorage was provided.

Most of the studies that were carried out earlier for seismic bond strengthening used “passive” confinement techniques. That is, techniques in which the effect of confinement is activated once splitting cracks initiate under the radial component of the bond forces. Because of its “passive” nature, experimental results clearly show that most of these techniques fell short of achieving the full potential of rectangular or circular columns that are originally designed for earthquake loads in accordance with recent versions of international codes of practice, such as AASHTO LRFD (2011). That is, columns that are splice-free, and at the same time adequately confined by closely spaced transverse steel ties, within the critical hinging region. Most of the strengthened column specimens in the various test programs, in which steel or CFRP jackets were used, performed well and better than as-built specimens up to drift ratios between $\pm 2.5\%$ and $\pm 4\%$, beyond which the columns suffered bond degradation and considerable slip of the spliced bars, leading to quick loss in lateral load capacity and significant pinching in the lateral load-drift response.

1.2 Review of Bond

The use of reinforced concrete as a structural material is due to the combination of the steel and concrete. When a load is applied, the strain in the steel at the level of the concrete is almost equal to the strain of the concrete at that same level. Steel is

strong and ductile in compression while the concrete is strong and durable in compression. The interaction between the two materials, which gives reinforced concrete a significant property, has to be maintained to create a composite reaction. This interaction is known as the bond strength and it allows for the transfer of load between concrete and steel. The stress transfer across the steel-concrete interface is one of the major factors affecting the bond strength. Such stress transfer results in a mutual adhesion between the two components. Other factors include the pressure exerted by the concrete on the reinforcing steel due to the drying shrinkage of concrete. Bond strength plays a major role in controlling the characteristics of reinforced concrete.

Steel bars are usually deformed into outer patterned ridges as illustrated in Figure 1 below. These deformations (lugs) contribute to the bond strength between steel and concrete through mechanical anchorage. Bond resistance mechanism is made up of three main components and they are mechanical interlocking between steel deformations and the surrounding concrete, friction forces on the steel-concrete interface surface, and chemical mutual adhesion between the two materials. Figure 1 illustrates these three components.

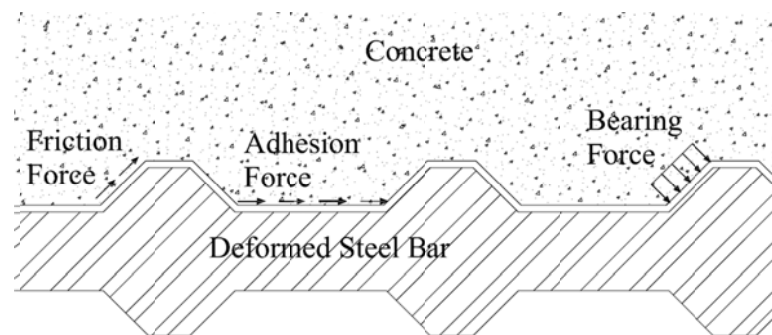


Figure 1. Steel-concrete bond resistance components

Two forms mainly characterize bond failure between steel and concrete and they are splitting bond failure and pull-out bond failure. If the concrete cover around the reinforcing bars is small enough, or the steel bars are closely spaced, bond failure occurs by splitting of the concrete around the reinforcing bars. However, if the concrete is well confined by transverse reinforcement or the concrete cover around the reinforcing bar is large enough, pull-out bond failure takes place as a result of the concrete keys shearing off between the lugs. The amount of confinement is an effective factor in bond strength between steel and concrete.

For most structural applications, bond failures are governed by splitting of the concrete rather than by pullout. The average bond strength at splitting bond failure is influenced by several parameters such as the ratio of concrete cover to bar diameter, the development or splice length, the concrete compressive strength and concrete confinement (Orangun, Jirsa, and Breen 1975).

1.3 Mechanism of Passive and Active Confinement

A common approach for seismic bond strengthening of lap-spliced reinforcement in existing RC columns is the use of external confinement, which include the use of steel jackets and the use of external carbon fiber-reinforced polymer (CFRP) jackets, and the use CFRP anchors. All studies conducted using these techniques have reported enhanced bond performance of the lap splices and improved seismic response of the columns.

However, confinement such as steel and CFRP jackets and CFRP anchors are all passive in nature. That is, their contribution to the bond resistance of tension lap splices

is utilized once splitting cracks initiate. This type of confinement does not fully prevent widening of the splitting cracks, particularly under large drift and splice stress reversals demanded by strong earthquakes. This justifies why most passively confined column specimens with lap splices developed enhanced seismic performance only up to drift ratios varying between 2.5 and 4%.

Also, because of slip of the spliced bars due to cyclic bond degradation, most of these specimens developed pinching in their lateral load-drift response and relatively low energy absorption and dissipation capacities. Add to this the fact that, because of their low stiffness against lateral dilation of concrete, passive confinement, especially CFRP jackets, are not as effective in confining spliced bars along the long side of rectangular columns with large aspect ratio (Kim et al. 2011; Hantouche and Harajli 2013) or when compared to columns with circular sections.

For wide rectangular RC columns with bending about their minor axis, Kim et al. (2011) proposed using a combination of CFRP jackets and CFRP anchors. However, once again, because of the cyclic bond degradation, the columns in the test of Kim et al. (2011) encountered pinching in the lateral load-drift response and experienced sharp drop in lateral load capacity at drift ratios varying between 3.0 and 4.0%.

Active confinement by means of pre-tensioned steel anchor rods is investigated in this research. Active lateral pressure on both sides of the specimen would suppress or prevent the development of splitting cracks for different bond design parameters, such as concrete cover, splice length, and concrete compressive strength. The concept of actively confining a column specimen is to apply lateral compression forces from both

sides of the minor axis within the splice region. This way splitting bond cracks will be arrested before they develop along the splice length.

CHAPTER 2

OBJECTIVE

In this study, the use of active confinement by means of pre-tensioned steel anchor rods for seismic bond strengthening of lap spliced reinforcement at the critical hinging region of rectangular or wall-type bridge piers is experimentally investigated. The test variables covered diameter of the spliced bars, ratio of the pier longitudinal reinforcement and configuration of the pre-tensioned steel anchor rods. A design procedure is developed for engineers for evaluating the minimum active lateral pressure required for adequate bond strengthening and for designing the strengthening system under investigation. A design example is provided to illustrate the use of the proposed procedure.

It should be mentioned that one of the main advantages of the current study is that it explores a new technique for seismic strengthening and rehabilitation of existing RC structures. Note that it is possible that RC bridge piers may require seismic retrofitting for preventing other modes of structural failure under axial, shear and/or flexural loads. However, this study concentrates on aspect of retrofitting, namely bond strengthening of deficient lap splices which is considered one of the most common causes of structural failure of RC bridge piers or columns in general under earthquake loading.

In summary, previous techniques for seismic bond strengthening of lap spliced reinforcement in circular or rectangular columns used passive confinement. Most of the

tried techniques succeeded in improving the seismic performance of bond-critical region in RC columns, but fell short of achieving the full potential of columns or bridge piers that are originally designed for earthquake loads in accordance with modern codes of practice.

Active confinement by means of pre-tensioned steel anchor rods for seismic bond strengthening of lap spliced reinforcement at the critical hinging region of wall-type bridge pier is experimentally investigated. The study is significant for (i) assessing the success of active confinement in improving the seismic behavior of gravity load designed RC columns or bridge piers having lap spliced reinforcement; and (ii) exploring new and more effective techniques for seismic strengthening and rehabilitation of existing RC structures when compared to other techniques reported in the technical literature.

CHAPTER 3

EXPERIMENTAL PROGRAM

3.1 Test Specimens

The specimens represent a typical small scale 65 cm wide strip of a RC bridge wall-type pier as shown in Figure 2. The pier is assumed to be subjected to longitudinal earthquake forces parallel to the axis of the bridge. Figure 3 shows details of the specimens. The effective height and section depth of the pier specimen are 150 cm and 25 cm, respectively, producing a reasonable height-to-depth ratio of 6.0. Note that the actual height of the specimen is 160 cm, however the lateral force was applied at a height of 150 cm, i.e. the effective height is 150 cm (see Figure 3) The pier strip (referred to as “column” or “pier”) is supported over a 100 cm long, 70 cm wide, and 40 cm deep footing. Table 1 provides a summary of the specimens’ designation, test parameters, and strengthening technique, if any.

The test variables included the reinforcement ratio of the columns, the bar diameter, and the configuration of the steel anchor rods. The specimens were divided into three test series, W16, W20, and W25 corresponding to diameters of the pier reinforcement of 16 mm, 20 mm, and 25 mm, respectively. The selected reinforcement areas produced reinforcement ratios (ratio of longitudinal steel area to the area of the pier gross section) close to 1.5% for W16, 1.9% for W20, and 2.4% for W25. The longitudinal reinforcements in all specimens were spliced at the column/pier base. The splice lengths were $35d_b$ or 56 cm for specimens W16, $35d_b$ or 70 cm for W20, and $46d_b$ or 115 cm for W25, where d_b is the bar diameter.

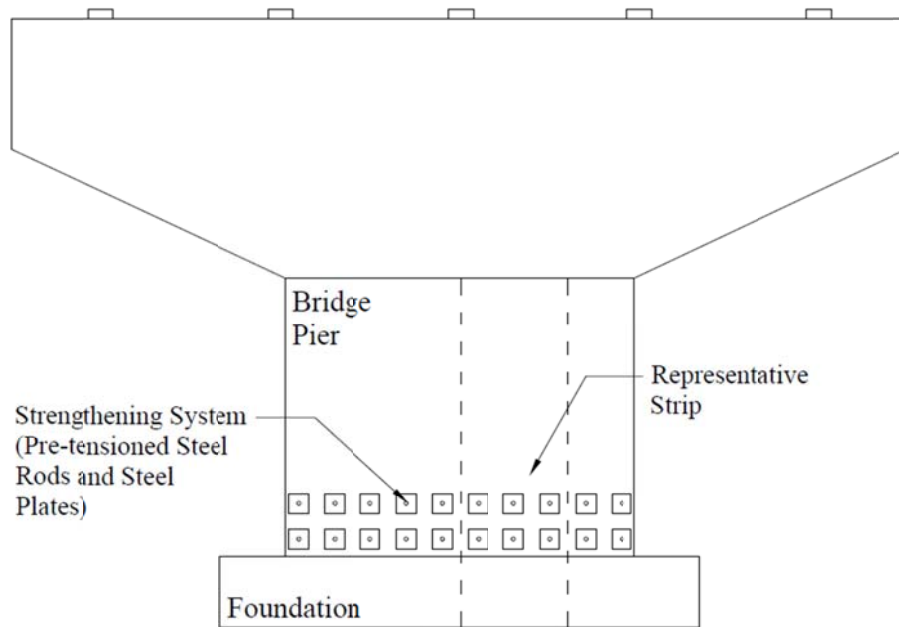


Figure 2. Proposed strengthening system for wall-type bridge pier

These splice lengths (for Series W16 and W20) were selected to conform to a great extent with the minimum length of tension splice of $36d_b$ specified in Section 1.5.3 of the 1973 version of AASHTO standard specification for Grade 60 steel. The transverse reinforcement consisted of one peripheral and one interior tie having $\phi 8$ mm in diameter and spaced 20 cm apart throughout the height of the specimens (see Figure 3). The starter bars were extended to the bottom of the footing and anchored using standard 90 degree hook. The spacing of the transverse reinforcement inside the footing was reduced to about 6 cm. The covers to the transverse steel ties on all sides of the column were maintained at 3 cm for all specimens.

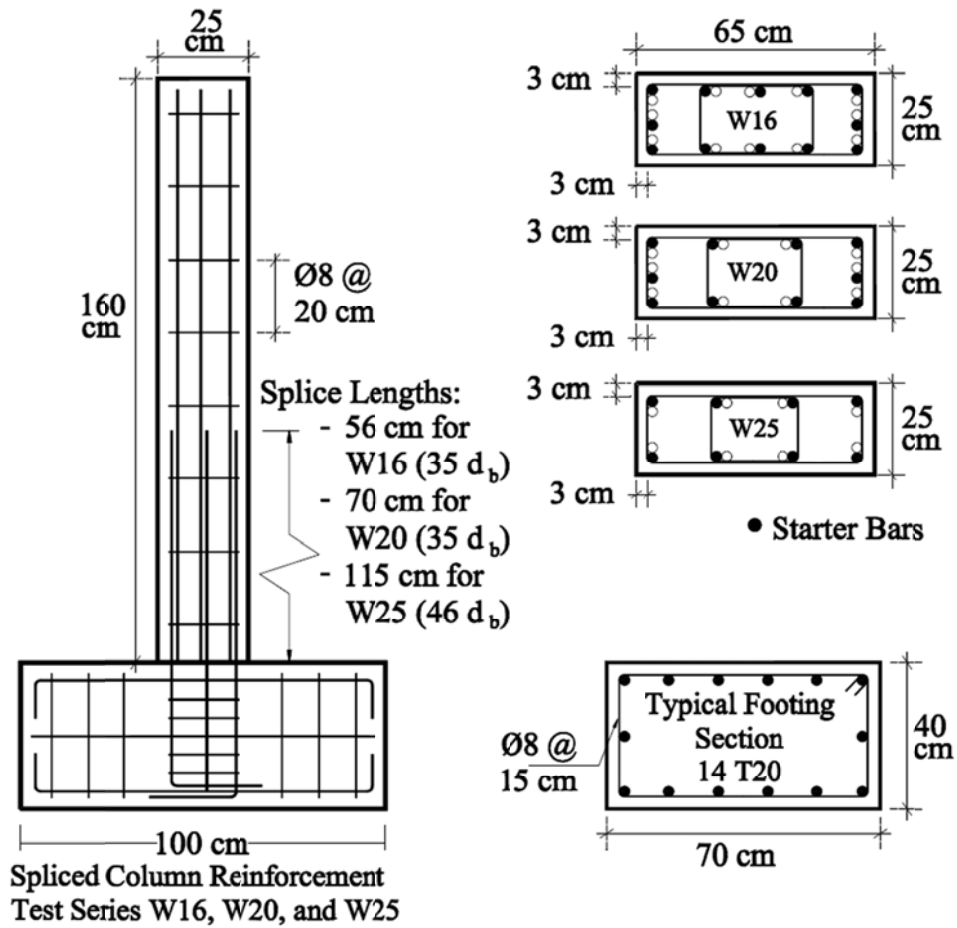


Figure 3. Dimensions and reinforcement details of the column specimens

Two categories of specimens were tested in each series. One as-built (W16-U, W20-U or W25-U) and one strengthened using active confinement by means of pre-tensioned steel anchor rods (W16-SA, W20-SA or W25-SA1, W25-SA2, W25-SA3). For series W16 and W20, one specimen was tested from the strengthened category, while for series W25, three specimens were tested, each with a different configuration of the pre-tensioned steel anchor rods.

Table 1: Specimens Notations and Strengthening Techniques

Specimen Series	Specimen Notation	f'_c (MPa)	Strengthening Technique
W16 $A_{st} = 12$ T16 $f_y = 570$ MPa $L_s = 560$ mm	W16-U	30.0	As-Built. No Strengthening
	W16-SA	32.0	9 steel anchor rods pre-tensioned using steel plates and bolts along the splice length. See Figure 5.
W20 $A_{st} = 10$ T20 $f_y = 608$ MPa $L_s = 700$ mm	W20-U	30.0	As-Built. No Strengthening
	W20-SA	32.0	9 steel anchor rods pre-tensioned using steel plates and bolts along the splice length. See Figure 5.
W25 $A_{st} = 10$ T25 $f_y = 608$ MPa $L_s = 700$ mm	W25-U	26.0	As-Built. No Strengthening
	W25-SA1	32.0	12 steel anchor rods pre-tensioned using steel plates and bolts along the splice length. See Figure 5.
	W25-SA2	26.0	12 steel anchor rods pre-tensioned using steel plates and bolts along the splice length. See Figure 5.
	W25-SA3	32.0	12 steel anchor rods pre-tensioned using steel plates and bolts along the splice length. See Figure 5.

The specimens of the second category were strengthened by applying lateral compression force on the concrete within the splice region. The compression force was attained by pre-tensioning through steel anchor rods placed inside predrilled holes and bearing against discrete steel plates in the position shown in Figures 5 and 6. The diameter of the anchor rods was determined based on the estimated rod pre-tension force required in each specimen for achieving “adequate” bond strengthening. The size of the steel bearing plates was selected to fully transfer the steel anchors pre-tension force to the concrete.



Figure 4. Lateral load applied at an effective height of 150 cm of the specimen.

The advantages of using discrete steel pates as opposed to continuous horizontal steel strips or complete steel jacket is that they are more economical, easier to manage, and allow more flexibility in construction, particularly when strengthening wide columns such as bridge piers or concrete walls. Also, the use of discrete steel plates does not increase the lateral stiffness of the columns, and therefore does not attract additional earthquake shear forces when compared with steel jackets.

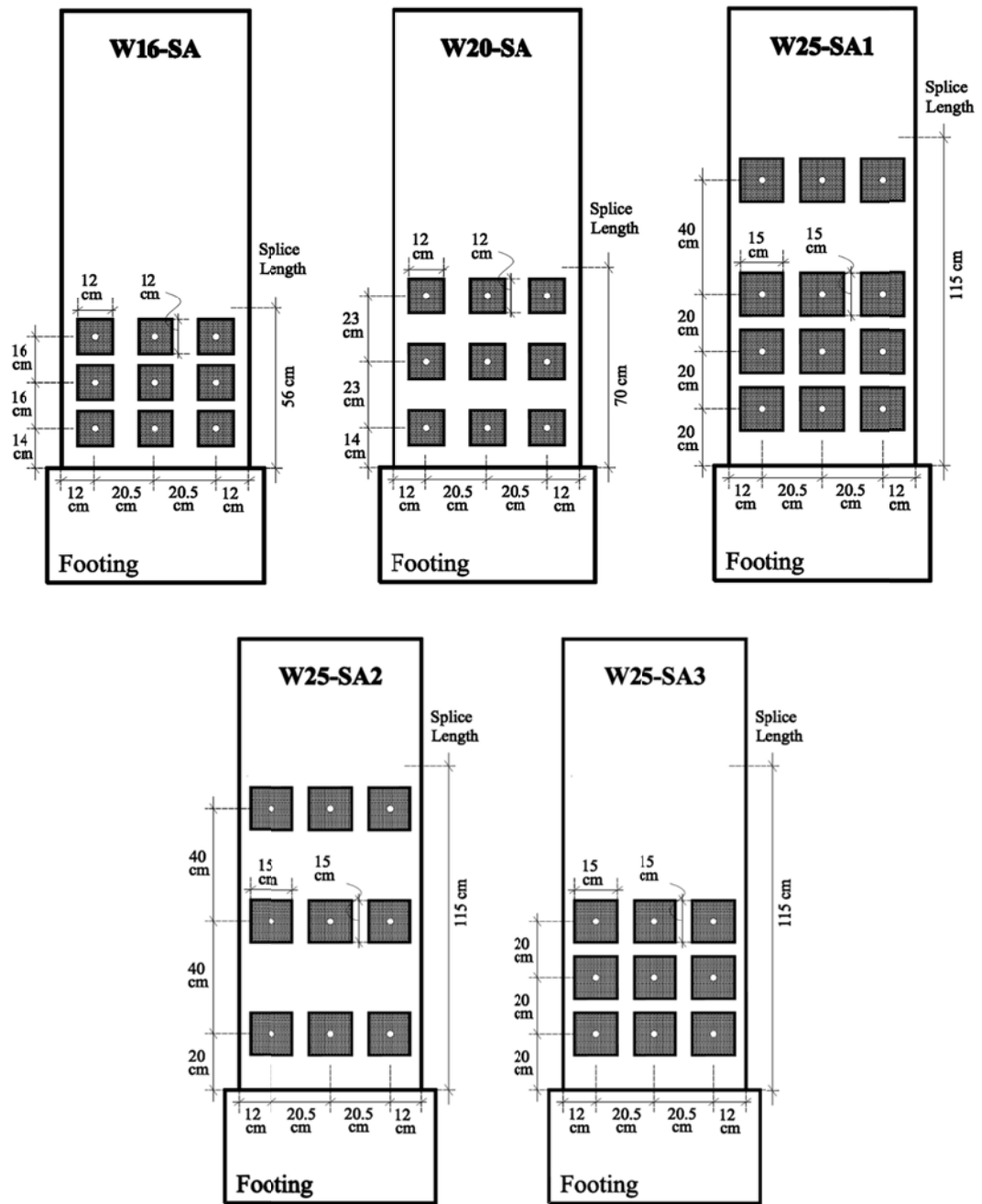


Figure 5. Steel anchor rods and steel plates configuration

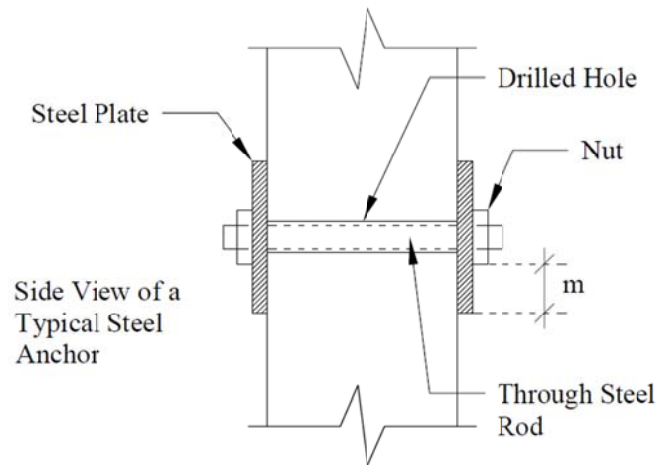


Figure 6. Side view of steel plates and anchor rods

3.2 Materials

3.2.1 Reinforcing Steel

Grade 60 reinforcing steel bars having actual yield strength of 570 MPa, 608 MPa, and 588 MPa for the 16 mm, 20 mm, and 25 mm steel bars were used as longitudinal reinforcement (See Table 1). The transverse reinforcement hoop stirrups used in the shear spans consisted of 8 mm Grade 60 spaced at 20 cm. The steel anchors consisted of 20 mm diameter threaded rods having Grade A325M steel with ultimate strength of 800 MPa and yield strength of 640 MPa. The bearing plates were A36 steel having yield strength of 248 MPa.

3.2.2 Concrete

The specimens were cast using ready-mix concrete. The mix proportions per cubic meter, for achieving a target compressive strength f'_c of 30 MPa, were 1,065 kg of 1 cm maximum size limestone coarse aggregate; 778 kg of a combination of crushed sand and natural sand; 375 kg of Portland cement type I; and 161 kg of water. The

actual 28-day concrete compressive strengths f'_c for the specimens are reported in Table 1, and they are based on the average compressive strength of five standard 15 cm diameter by 30 cm long concrete cylinders taken from each batch.

3.3 Construction of Specimens

3.3.1 Formwork

The formwork unit consisted of two parts, the footing and the column. The footing has a dimension of $100 \times 75 \times 40$ and the column has a dimension of $160 \times 65 \times 25$ both in centimeters. To maintain a constant width of the column along its length and to ensure the rigidity of the form during casting, top wooden braces were provided as can be seen in Figure 7. Spaces between formwork units were sealed before casting to ensure water-tightness of the forms.



Figure 7. Formwork with top wooden braces before and after casting

3.3.2 Fabrication of Cages

The steel cages of the footings and the columns were fabricated separately and then joined before being placed in the form work. Steel wires were used to fix the bars together and provide the required splice length.

3.3.3 Casting

As mentioned before ready-mix concrete was used, and the procedure was the same for all specimens. Three different concrete batches were, however the specimens strengthened using active confinement by means of pre-tensioned steel anchor rods, were all cast at the same time using one concrete batch. Five cylinders were taken from each batch. Table 1 provides the average values of the concrete compressive strength tested after 28 days after casting.



Figure 8. Formwork removed and specimen is erected

During casting laboratory vibratos were used to ensure the homogeneous consolidation of the concrete, reducing air-entrapment. At the end of the casting procedure, the top surface of the specimen was smoothed and lifting hooks were inserted. Both the specimens and the testing cylinders were sprayed with water for 3 days continuous to ensure curing of the concrete. After this, the specimens were erected and the formwork removed as shown in Figures 8 and 9.



Figure 9. Specimen erected

3.4 Loading Procedure and Instrumentation

Loading of the specimens was conducted at least 28 days after casting. The specimens were supported on a strong reinforced-concrete floor, whereby the footing was fixed to the ground using two steel beams. Four steel plates were tightened to the beams and tightened with two bolts each to avoid any sliding of the specimens during loading. A reinforced-concrete reaction wall was used with 250 kN capacity actuator to apply the lateral load. The actuator was aligned horizontally and checked using a mercury leveler to apply the lateral force on the required location and maintain it throughout the loading procedure. The load applied by the hydraulic actuator was centered at 150 meters above the column base. Figure 10 below demonstrates the whole loading setup used as described above, while Figures 11 and 12 were taken during an actual loading test carried out on specimen W20-SA.

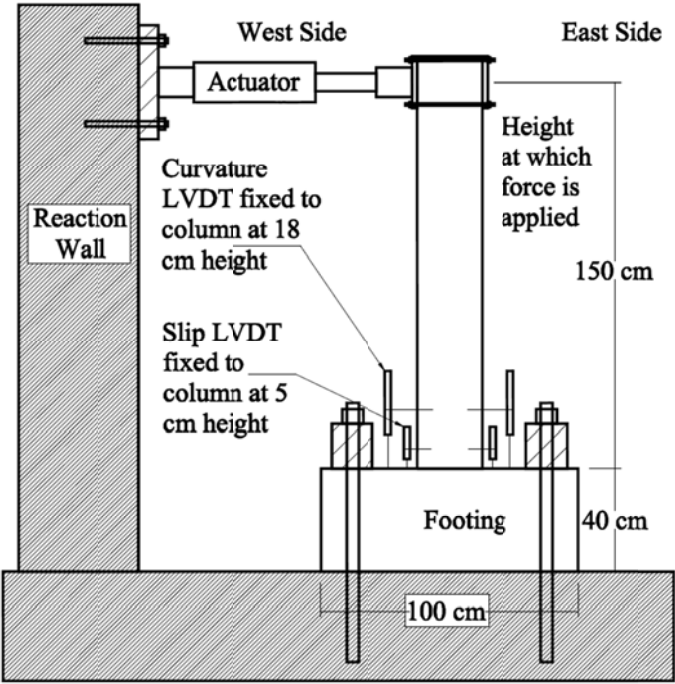


Figure 10. Loading setup



Figure 11. Actual load testing carried out on Specimen W20-SA.



Figure 12. Maximum push cycle causing specimen W20-SA to tilt.

All columns are supported on a RC strong floor and loaded as shown in Figure 4 through a RC reaction wall. All specimens were subjected to the same loading protocol shown in Figure 13 below. The loading protocol is composed of a sequence of displacement-controlled cycles given in percent lateral drift, or drift ratio [DR = $(\Delta_1/h_0) \times 100\%$], where Δ_1 is the lateral drift and h_0 is the height of the column at the point where the lateral load is applied. In order to simulate the actual cyclic loading condition, the load was composed of a sequence of displacement-controlled cycles using 1 point loads in accordance with the cyclic load history shown in Figure 13 below, the exact drift ratio with its corresponding cycle number are shown in Table 2.

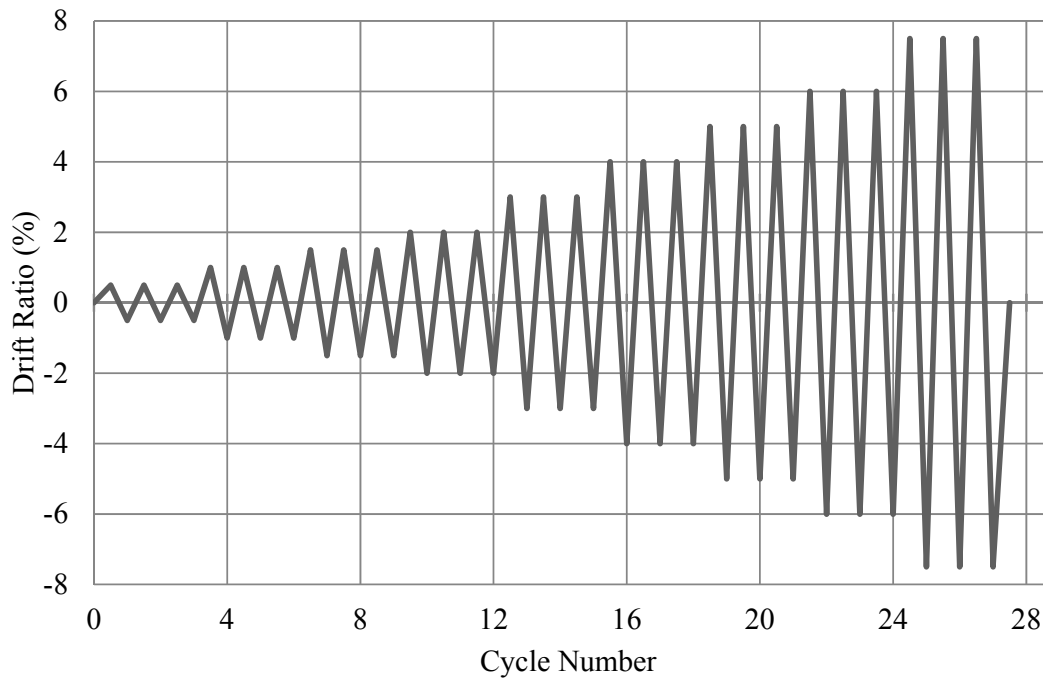


Figure 13. Loading protocol

For the strengthened specimens, W16-SA, W20-SA, and W25-SA, each anchor rod was fastened against a steel plate using a steel nut from one side and pre-tensioned

against another steel plate from the other side. Pre-tensioning of the rods was carried out one day or immediately before loading. The design pre-tension force was acquired using a torque-meter and monitored simultaneously using strain gages mounted on four rods before they were installed inside the holes.

Table 2. Drift ratio, amplitude and its corresponding cycles

Drift Ratio (%)	Amplitude (mm)	cycle
0.50	7.5	1
		2
		3
1.00	15.0	4
		5
		6
1.50	22.5	7
		8
		9
2.00	30.0	10
		11
		12
3.00	45.0	13
		14
		15
4.00	60.0	16
		17
		18
5.00	75.0	19
		20
		21
6.00	90.0	22
		23
		24
7.50	112.5	25
		26
		27

It should be noted that because the concentration in this study is on the bond resistance of spliced reinforcement which depends primarily on the splice tension stress, the specimens were tested under pure flexural load. That is, the application of axial load on the columns was deemed to have little influence on the outcome of this study.

Test measurements included applied lateral load and lateral drift, rotation within 50 mm and 180 mm at the bottom of the column , strain in the outermost column reinforcement (starter bars) at the column base, and increase in strain in the anchor rods. The test results were recorded using a data acquisition and control system.

The rate of lateral displacement was set at 2 mm per second, and was controlled manually from 0% to 100% of that set value. The test results were recorded using a data acquisition and control system. The system included sixteen channels which were connected to the strain gages on the steel reinforcement and the external linear variable differential transducers (LVDT). Two LVDTs that were used to measure the bond slip were located 5 cm from the top of the footing and located near the center of the face of the column. Another two LVDTs located next to the former ones but at 18 cm from the top of the footing were used to measure the curvature (See Figure14).



Figure 14. Steel plates configuration and wiring connections of the strain gauges for specimen W20-SA

A channel was dedicated to measure the hydraulic load given by the machine and another used to measure the lateral displacement of the column which is the axial displacement of the actuator at the point of the applied force.

CHAPTER 4

DESIGN GUIDELINES

4.1 Guidelines

Bond failure of steel bars occurs either in splitting mode or pullout mode. If the concrete cover is relatively small and/or the concrete surrounding the developed/spliced bar is not well confined, bond failure occurs by tension splitting of the concrete under the radial component of the bond forces. On the other hand, if the concrete cover is large, and/or the concrete is well confined, bond failure occurs in pullout mode before the development of splitting cracks by shearing off the concrete keys between the bar deformations (lugs). In normally detailed RC members (normal concrete covers, splice lengths, and areas of transverse steel confinement) the bond force required to shear off the concrete keys between the bar lugs is sizably larger than that required to cause tension splitting in the surrounding concrete. Consequently, bond failure in most RC members occurs in splitting mode.

The design strategy of the strengthening system used in this investigation is based on the concept of transforming the bond resistance of the lap spliced bars from splitting mode to pullout mode by applying lateral pressure that would completely suppress the bond splitting cracks before they develop. Transforming the bond resistance from splitting mode to pullout mode improves the bond performance of the spliced bars by restraining, or at least reducing, bond degradation associated with the progressive widening of the splitting cracks under drift and splice stress reversals.

One of the earliest studies for evaluating the effect of lateral pressure on bond strength of steel bars in tension goes back to 1965 (Untrauer and Henry). Since then, several additional experimental studies have been carried out. A concise summary of test results were reported and discussed by Eligehausen et al. (1983), and more recently by Xu et al. (2014). Most of these studies, which were conducted using short bar embedment lengths with pullout mode of bond failure, reported increase in the pullout bond strength with increase in lateral pressure. However, at present, there is no easy design approach for quantifying the minimum active lateral pressure that would modify the mode of bond failure from splitting mode into pullout mode for different bond design parameters, (ex. concrete cover, splice length, concrete compressive strength). Kim et al. used the shear friction concept for calculating the area of FRP transverse anchors required for bond strengthening of spliced reinforcement in RC columns. If a similar concept is to be used in this study, albeit the splice arrangement (lateral) used in the current test program is different from the splice arrangement (radial) used by Kim et al., the hypothetical shear plane shown in Figure 15 will be assumed to transfer a total splice force T_b corresponding to the development of some desired splice stress f_s .

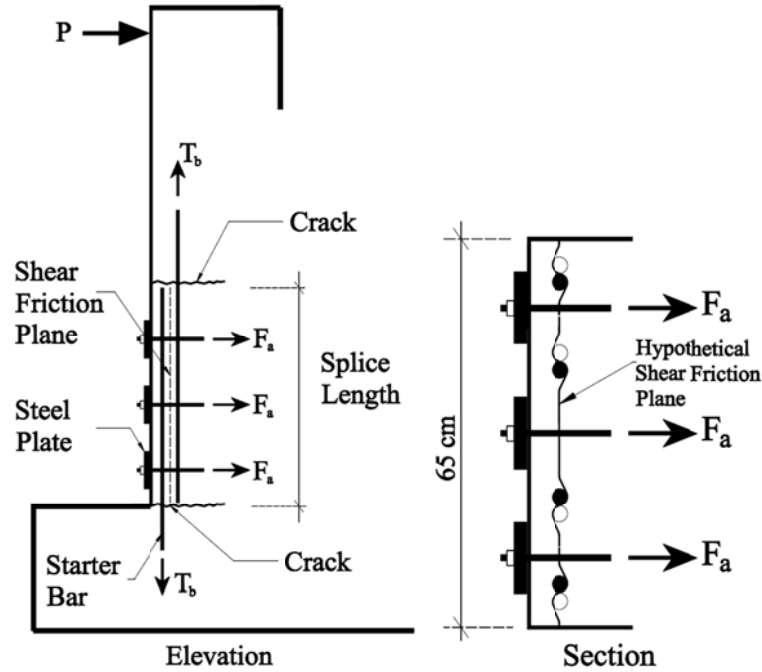


Figure 15. Shear friction concept for evaluating the anchor pre-tension force

In most cases, the actual yield strength of steel reinforcement is larger than the design yield strength. Therefore, for seismic bond strengthening, in order to avoid bond splitting failure due to large steel stresses or strains that are normally demanded by strong earthquakes, it was recommended (El Souri and Harajli 2011) to use a splice stress f_s equal to either $1.25 f_y$ (actual) or $1.85 f_y$ (design), which is in line with the recommendation made earlier by Hawkins et al. (2000). Neglecting, conservatively, the contribution of the internal steel ties crossing the shear plane to the shear friction resistance, and setting force equilibrium along the shear plane between the tension force T_b in the spliced bars and the shear friction force produced by an actively applied compression force F_1 on the shear plane (equal to the pre-tension force in the steel rods) leads to the following:

$$\mu F_l = 1.85 n_s A_b f_y \quad (1)$$

Where A_b is area of one spliced bar, f_y is design yield strength and n_s is the number of spliced or starter bars; μ is coefficient of friction, taken as 1.4 in accordance with ACI 318-11. The force F_l is thus calculated as:

$$F_l = \frac{1.85n_s A_b f_y}{\mu} \quad (2)$$

It can be easily verified that the force F_l calculated using Equation (2) is equal to 550 kN, 690 kN, and 1080 kN for each of the specimens in test series W16, W20 and W25, respectively.

However, a more realistic but yet approximate approach for estimating F_l , which takes into account most of the design parameters that influence the bond strength, would be to use the following basic and well known expression developed by Orangun et al. (1977) for calculating the average bond strength u_a at bond failure of steel confined concrete:

$$\frac{u_a}{\sqrt{f'_c(\text{MPa})}} = 0.1 + 0.25 \frac{c}{d_b} + 4.15 \frac{d_b}{L_s} + \frac{A_{tr} f_{ytr}}{41.6 s n_s d_b} \quad (3)$$

in which c is minimum concrete cover and L_s is splice length; A_{tr} , s and f_{ytr} are area, spacing, and yield strength of transverse steel reinforcement crossing the potential plane of splitting. By making analogy between the anchor lateral force and the force developed in the transverse steel reinforcement at bond failure, the term $A_{tr} f_{yt} / s$ can roughly, but conservatively, be replaced by the total active anchor force F_l per unit length along the splice length, i.e., $A_{tr} f_{yt} / s = F_l / L_s$, required to develop a splice tension force equal to $A_b (1.85 f_y)$ at bond failure. Using equilibrium between the splice force and the bond force for one spliced bar, i.e., $A_b (1.85 f_y) = u_a \pi d_b L_s$ in which $A_{tr} f_{yt} / s$ in Equation (3) is substituted by F_l / L_s , and neglecting the contribution of the

internal steel ties to the bond resistance, leads to the following expression for estimating the total lateral active force F_l within the entire splice region of the column:

$$F_l = 41.6n_s L_s d_b \left[\frac{1.85A_b f_y}{\pi d_b L_s \sqrt{f'_c}} - \left(0.1 + 0.25 \frac{c}{d_b} + 4.15 \frac{d_b}{L_s} \right) \right] \quad (4)$$

Using Equation (4) and considering a design concrete compressive strength $f'_c = 30\text{MPa}$, the values of F_l were calculated at approximately 350 kN for specimen W16, 720 kN for W20, and 920 kN for W25, respectively, which are coincidentally of the same order of magnitude as those estimated from Equation (2). Note that Equation (4) predicts an increase in F_l as the concrete cover, splice length, or concrete compressive strength decreases.

The number of steel anchor rods depends on the selected dimension B of the steel plates. The corresponding dimension B (assuming square plates) can be chosen such that the entire concrete cover plane A-A within the splice region (Figure 16) is under uniform compression stress, assuming the compression force in concrete propagates at a slope of 1:2 (AASHTO LRFD 2011). The minimum size B of the steel plate should also be adequate to prevent concrete bearing failure within some desired safety factor. The diameter d_a of the pre-tensioned steel anchor rods and the thickness of the steel bearing plates t_p are determined using Load and Resistance Factor Design (AASHTO LRFD, ANSI/AISC 2011):

$$d_a = \sqrt{\frac{4LF F_a}{\pi\phi_a F_{ya}}} \quad (5)$$

$$t_p = \sqrt{\frac{4F_a}{3f_b}} \quad (6)$$

Where F_a is the applied pre-tension force per one anchor rod, which is equal to the total force F_l divided by the number of anchor rods used within the splice region, and f_b is the allowable bending steel stress in the plate.

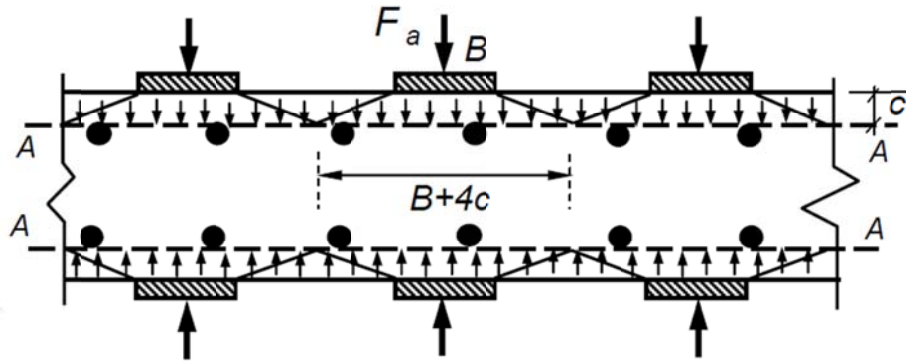


Figure 16. Concrete pressure distribution using active confinement

Guided by the aforementioned design criteria, nine steel anchor rods were selected for each of the strengthened specimens in series W16 and W20, and 12 rods for W25 (see Figure 3). The steel plates were all square having the following dimensions: $B = 12\text{cm}$ and thickness $t_p = 2\text{cm}$ for specimens W16 and W20; and $B = 15\text{cm}$ and $t_p = 2.5\text{cm}$ for W25. In all strengthened specimens, the pre-tension force F_a per one anchor rod was selected as 60 kN for W16, 80 kN for W20, and 110 kN for W25.

4.2 Design Example

Assume the bridge pier of Figure 1 has an overall width $W = 3500$ mm. The pier longitudinal reinforcement consists of two curtains of 25 mm diameter bars, spliced side-by-side with starter bars of the same diameter at a splice length $L_s = 30d_b = 760$ mm. The spliced bars are spaced horizontally at 150 mm, producing a clear horizontal spacing $c_h = 100$ mm and total number of splices $n_s = 24$. Bottom cover of longitudinal

reinforcement $c_b = 40$. Concrete compressive strength $f'_c = 30$ MPa, and design yield strength of the steel bars $f_y = 415$ MPa. The steel plates to be used are ASTM A572 Grade 50 having a yield strength $F_{yb} = 50$ ksi (345 MPa), while the pre-tensioned rods are ASTM F1554 high strength steel having a yield strength $F_{ya} = 105$ ksi (724 MPa). The load factor LF is assumed to be 1.4.

4.3 Design Steps

1. Estimate the total lateral force from Equation (4) to be $F_l = 10,055$ kN
2. Use trial and error to find the best combination of the number N_p and the size B of square plates, such that the thickness of the plate and the diameter of steel through rods are within practical design applications. Using the confinement concept shown in Figure 5, a straightforward relation between the size B and number N_0 of the steel plates or anchor rods per one row is expressed as:

$$N_0(B + 4c_b) = W \quad (7)$$

Using Equation (7), the following combination is selected: $B = 200$ mm, and $N_0 = 10$.

3. Determine the total number of plates N_p (or steel anchor rods) such that the strengthening system has at least two rows of anchor rods and such that $n_r(B + 4c_b) \leq L_s$, where n_r is the number of rows used. Using two rows leads to $N_p = 20$, and therefore the pretension force per one steel rod $F_a = F_l/N_p = 503$ kN.
4. Calculate the diameter d_a of the threaded steel rod using Equation (5) considering $\phi_a = 0.9$: $d_a = 37$ mm.

5. Calculate the thickness t_p of the steel plate from Equation (5) assuming the distance m from the edge of the steel plate to the face of the nut (Figure 3) = 70 mm, and considering $\phi_f = 0.9$: $t_p = 24$ mm.
6. Check bearing strength F_b under each of the plates (AASHTO LRFD):

$$F_b = 0.85\phi_b f'_c B^2 \left(\sqrt{\frac{(B + 4c_b)^2}{B^2}} \leq 2.0 \right) \quad (8)$$

where the load resistance for bearing $\phi_b = 0.7$. This leads to $F_b = 1285$ kN, which is larger than the factored applied force $LF \times F_a = 704$ kN.

CHAPTER 5

TEST RESULTS AND ANALYSIS

Application of load initially causes a lateral drift of the specimens away from the RC reaction wall. Throughout the discussion that follows, the west and east side of the columns correspond to the side close to or away from the reaction wall, respectively (see Figure 11). Table 3 below provides relevant test parameters and results obtained for the different test series.

Table 3. Relevant test parameters and results

Test Series	Specimen	f'_c (MPa)	P_{max} (kN)	DR_y (%)	DR_u (%)	μ_d (*)	Steel Tension Strain at P_{max} ($\mu\epsilon$)	
							Push Cycle	Pull Cycle
W16 $A_{st} = 12$ T16 $f_y = 570$ MPa $L_s = 560$ mm	W16-U	30.0	82.8	1.75	4.1	2.3	7400	12300
	W16-SA	32.0	96.0	2.1	>7.0	>3.3	10000	12000
W20 $A_{st} = 10$ T20 $f_y = 608$ MPa $L_s = 700$ mm	W20-U	30.0	99.0	2.1	5.7	3.1	2540	4400
	W20-SA	32.0	110.0	2.2	>7.5	>3.4	4200	4800
W25 $A_{st} = 8$ T25 $f_y = 588$ MPa $L_s = 1150$ mm	W25-U	26.0	122.7	2.4	5.2	2.2	4040	3700
	W25-SA1	32.0	139.3	2.2	>7.5	>3.4	4700	8500
	W25-SA2	26.0	136.5	2.3	>7.5	>3.3	3600	4000
	W25-SA3	32.0	139.3	2.2	>7.5	>3.4	5000	4500

(*) Average between compression and tension cycles

5.1 General Behavior and Mode of Failure

Flexural cracks developed in all specimens, as-built and strengthened, at the interface between the column and the footing (base of the column). The average spacing of the cracks for all specimens ranged from 20 cm to 30 cm. No shear cracks were witnessed during the testing procedure. The cracks were recorded using a pen during the testing, so that small cracks that might close and become invisible after testing will be recorded. Figure 17 demonstrate this process, Figures 18 to 23 show the final cracks map of the specimens, with an actual shot of each specimen after testing.

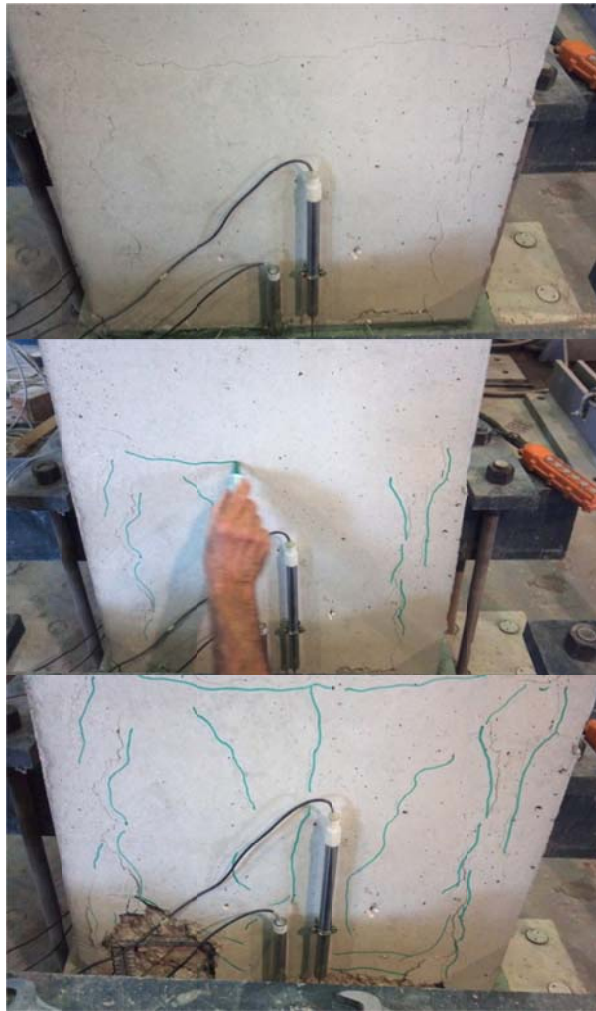


Figure 17. Crack path recording on W16-U specimen, during testing

The three as-built specimens (W16-U, W20-U, and W25-U) developed splitting cracks immediately after yielding of the starter bars. Bottom and side splitting cracks initiated at the corner spliced bars first, followed by bottom splitting developing in the intermediate bars. Splitting cracks initiated at the base of the columns and then propagated upward along the splice length as the lateral drift increased, causing spalling of the concrete (particularly in specimen W25-U), substantial slip of the starter bars, and concentration of deformation and widening of a major crack at the base of the column. The final failure mode for all as-built specimens was a combination of bond splitting and flexural failure associated with concrete crushing (compression failure) at the base of the column.

All strengthened column specimens (W16-SA, W20-SA, and W25-SA) developed minor splitting cracks with increase in lateral drift ratio beyond about ± 3.0 to $\pm 4.0\%$, and after yielding of the starter bars. These cracks, which concentrated close to the corner bars were hairline, and propagated only a limited distance above the base of the column. No side splitting was developed for the corner bars as occurred in the as-built specimens. The final failure mode of the strengthened specimens was a clear flexural failure associated with steel yielding and concrete crushing at the base of the column with concrete damage concentrating mainly within 40 mm to 60 mm above the column-footing interface.

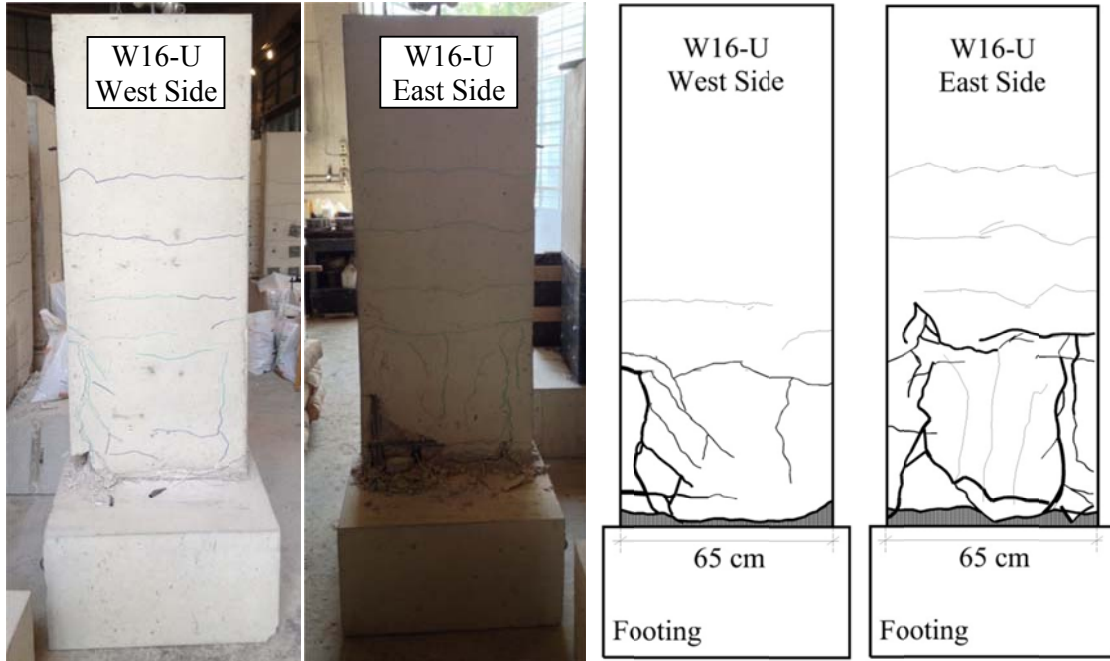


Figure 18. Crack distribution in the as-built specimens of series W16

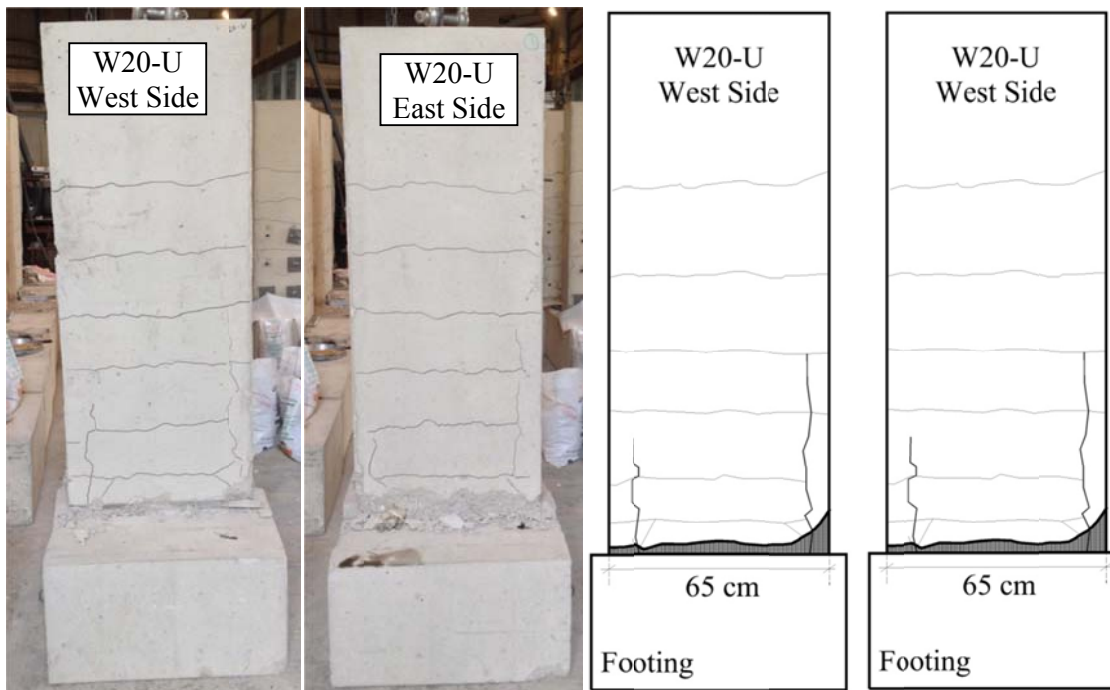


Figure 19. Crack distribution in the as-built specimens of series W20

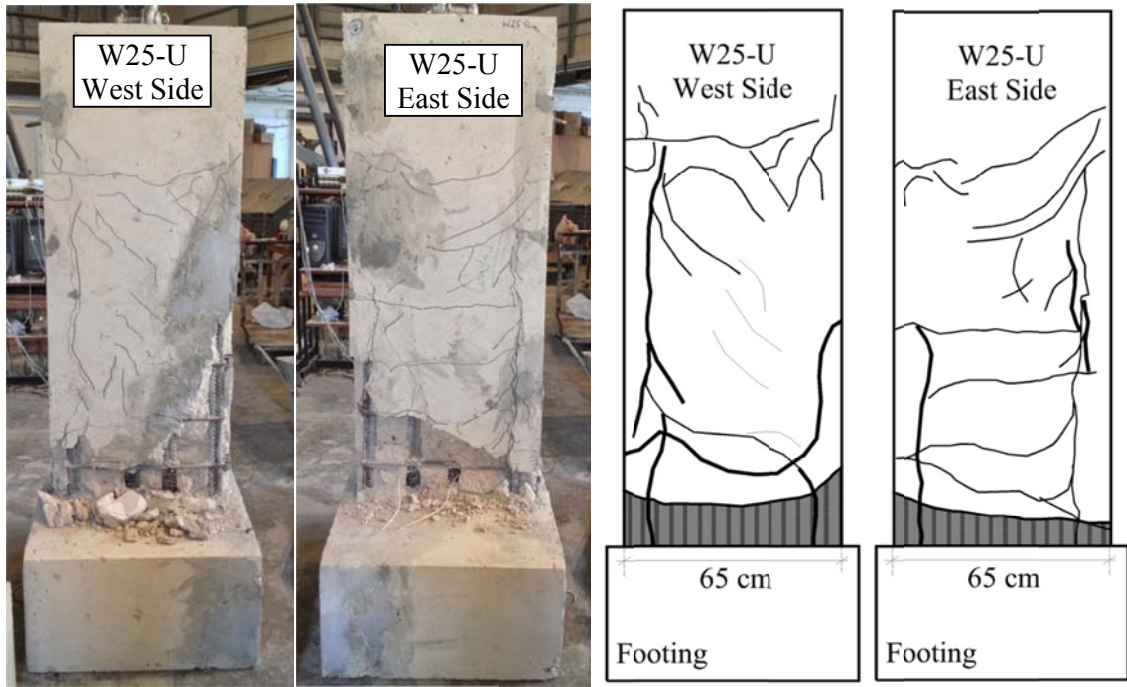


Figure 20. Crack distribution in the as-built specimens of series W20

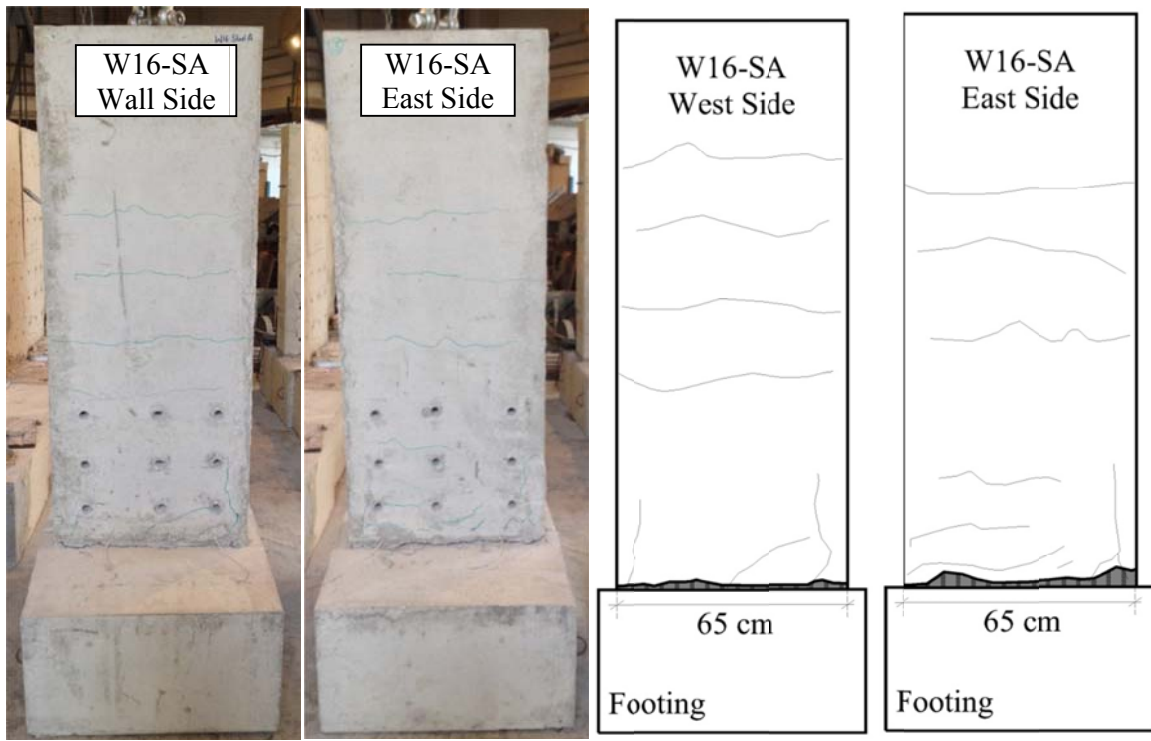


Figure 21. Crack distribution in the strengthened specimens of series W16

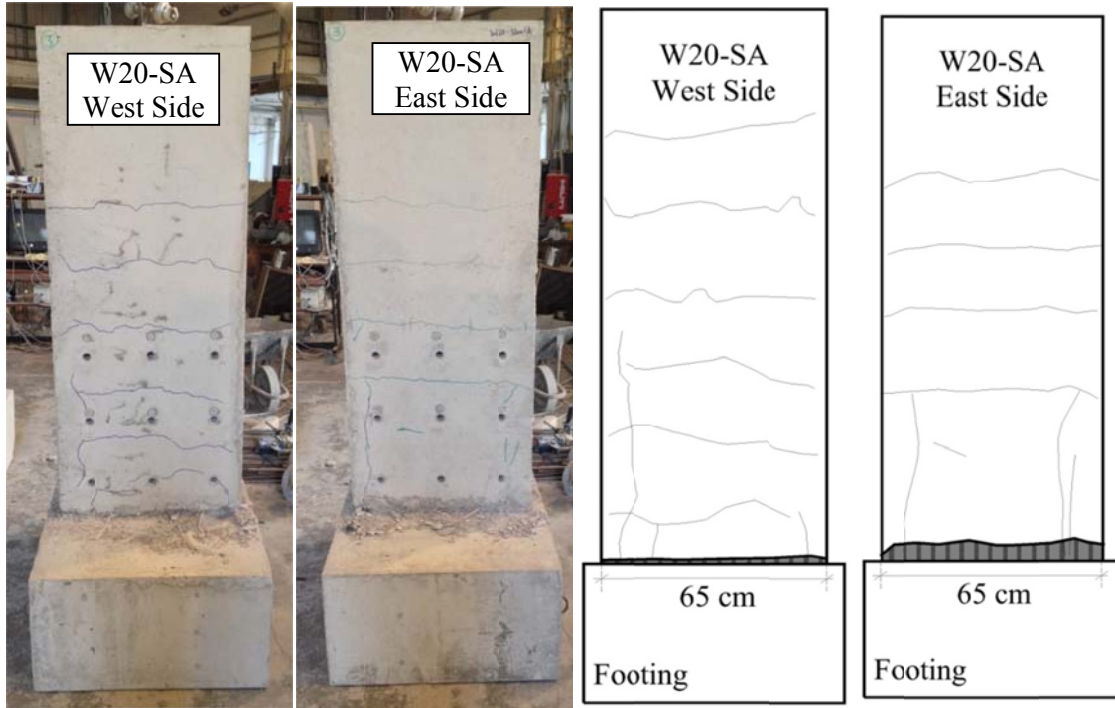


Figure 22. Crack distribution in the strengthened specimens of series W20

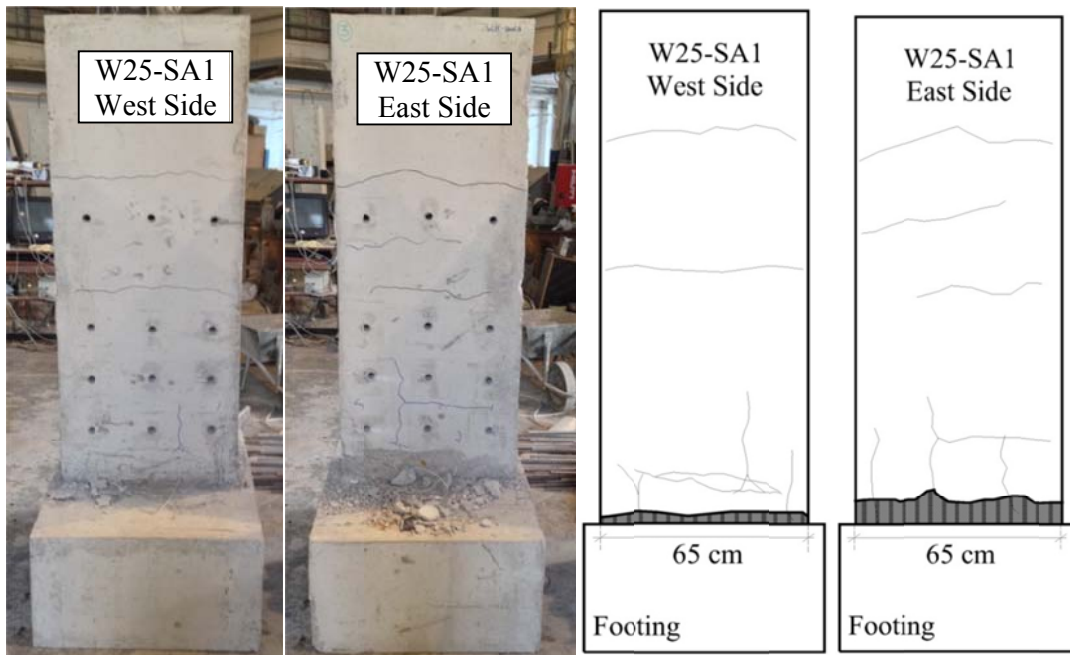


Figure 23. Crack distribution in the strengthened specimens of series W25

Examination of the lap-splice zone of the steel anchor bolted columns by removing the steel plates at the end of the test showed that these specimens did not experience any failure due to pre-stressing of these plates, and that concrete was still intact in these locations. Splitting bond failure was evident for all strengthened specimens, propagating to the around 50% of the splice region for the outermost reinforcements in specimens W16-SA and W25-SA, and to the full splice length in specimens W20-SA.

5.2 Lateral load-drift Response

Figures 24 to 29 show the applied column lateral load versus drift ratio response of the as-built and the strengthened column specimens in the three test series, W16, W20, and W25. A summary of the average envelope peak lateral loads P_{max} (average between the compression and tension cycles) attained by the various specimens is provided in Table 3.

5.2.1 As-built Columns

In all as-built specimens W16-U, W20-U and W25-U, yielding of the starter bars developed at drift ratios (average between the compression and tension cycles) of $\pm 1.75\%$, $\pm 2.1\%$ and $\pm 2.4\%$, respectively. Yielding of the starter bars was followed shortly by the development of bond splitting cracks. The development of splitting cracks combined with drift and splice stress reversals caused progressive bond deterioration and slip of the spliced bars, leading to gradual degradation of the flexural stiffness, drop in lateral load capacity, and significant pinching in the lateral load-drift response of the specimens towards the end of the test or a drift ratio of $\pm 7.5\%$.

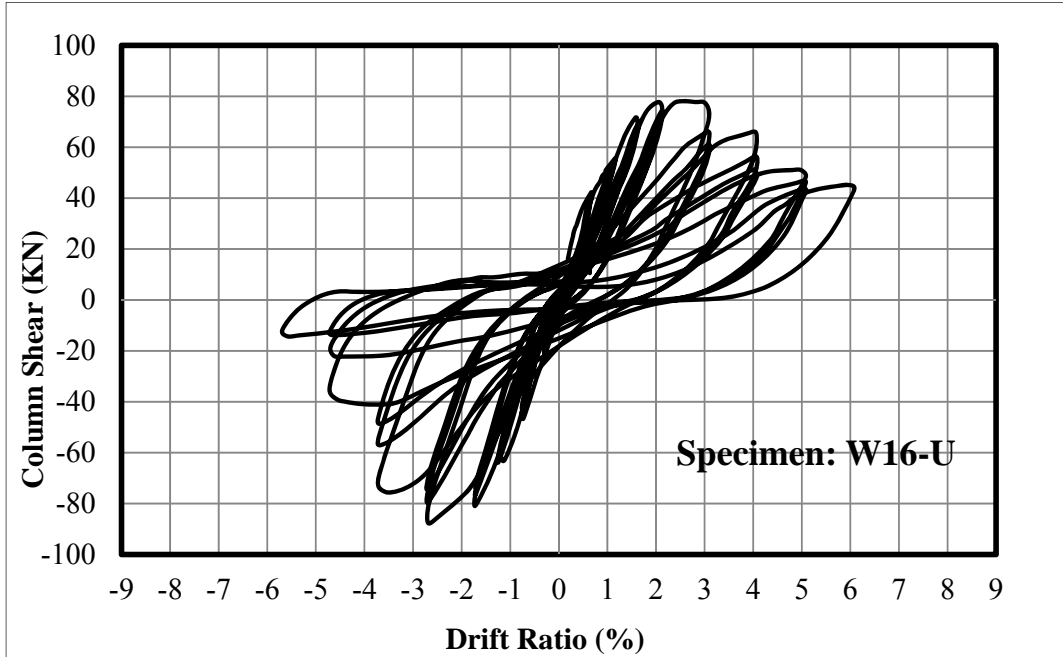


Figure 24. Lateral load-drift response for the as-built specimens in series W16

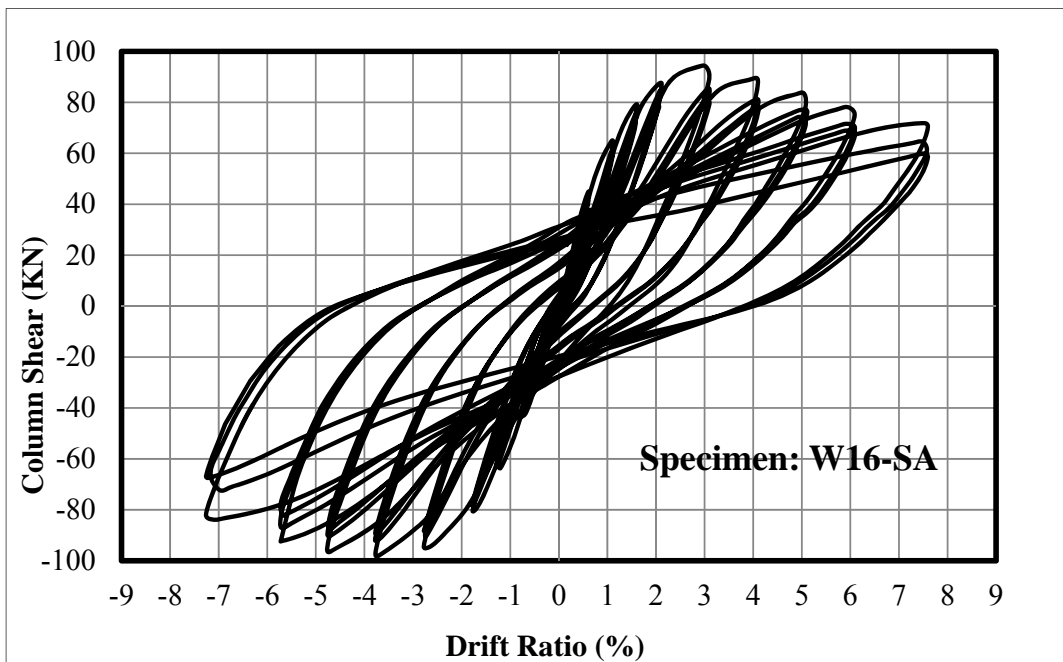


Figure 25. Lateral load-drift response for the strengthened specimens in series W16

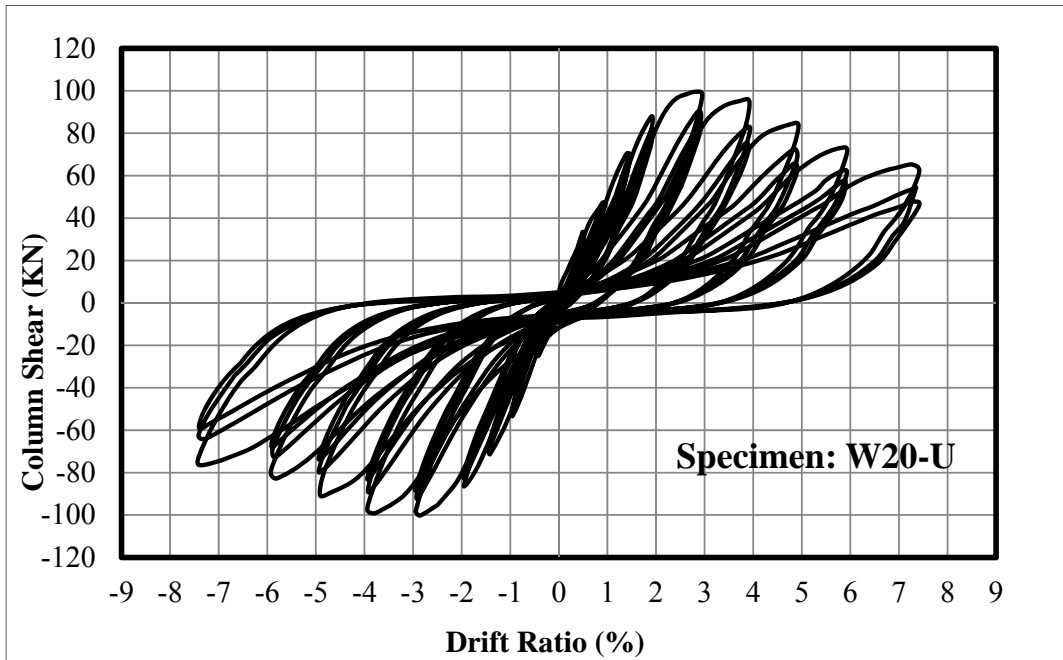


Figure 26. Lateral load-drift response for the as-built specimens in series W20

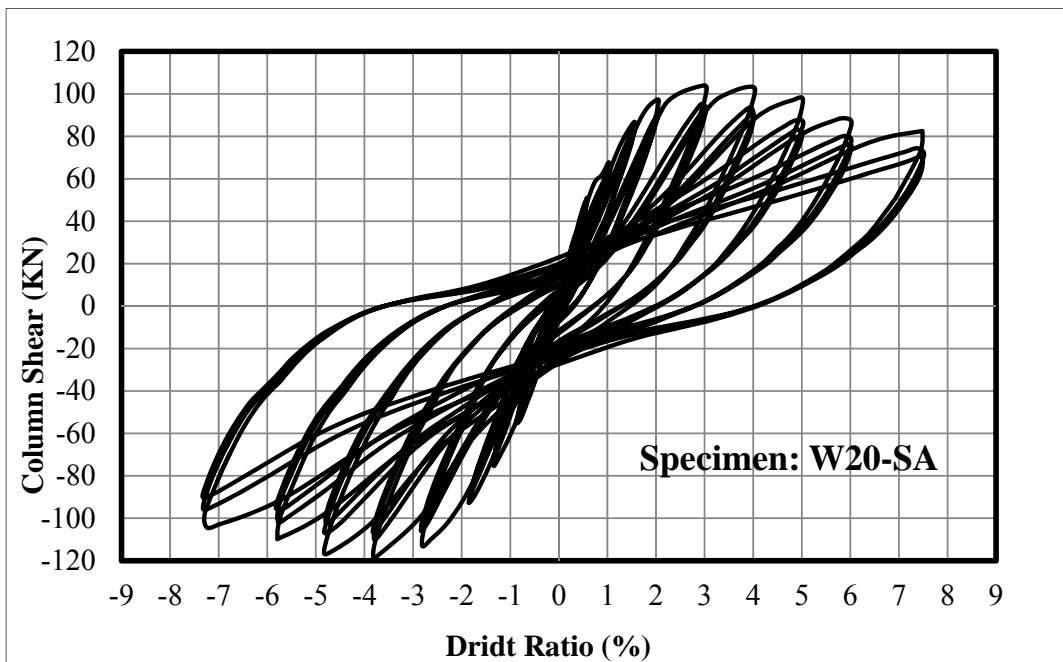


Figure 27. Lateral load-drift response for the strengthened specimens in series W20

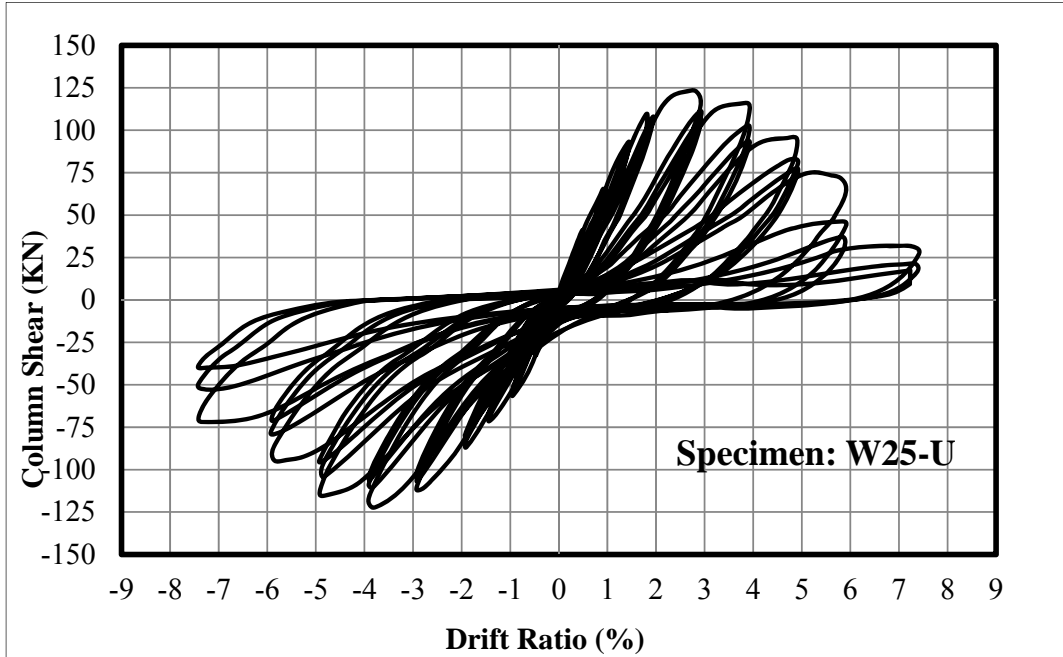


Figure 28. Lateral load-drift response for the as-built specimens in series W25

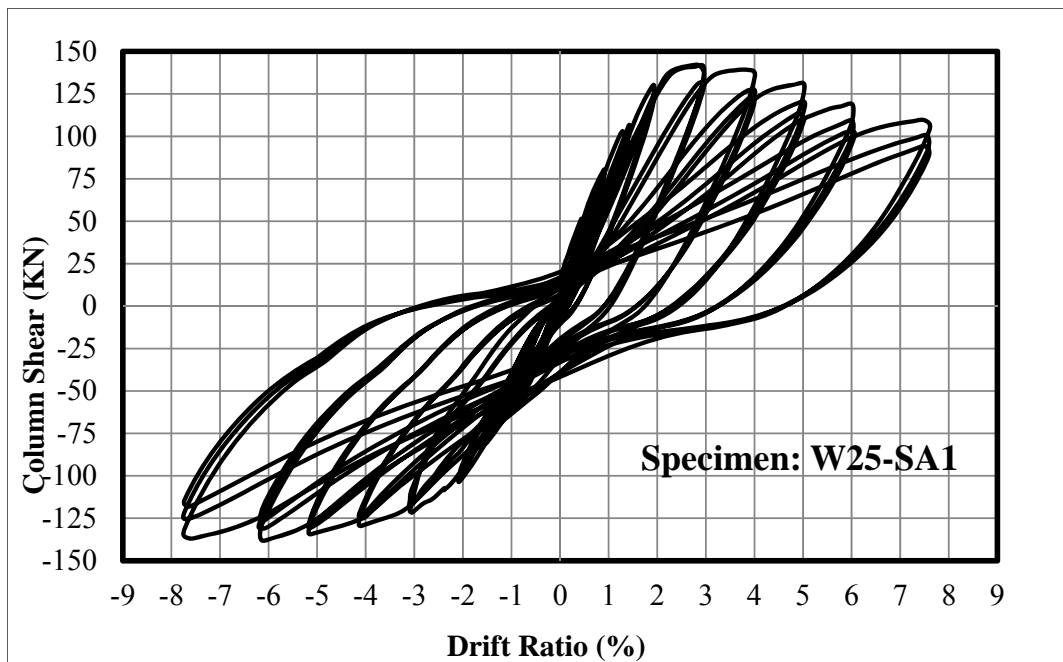


Figure 29. Lateral load-drift response for the strengthened specimens in series W25

The ultimate drift capacities of the specimens, defined as the drift at which the lateral load capacity drops to 80% of the peak lateral load, are summarized in Table 3. The corresponding capacities attained $\pm 4.1\%$, $\pm 5.7\%$ and $\pm 5.2\%$, for specimens W16-U, W20-U and W25-U, respectively. The displacement ductility, defined as the ratio of the ultimate drift ratio to the yield drift ratio, varied for the three as-built specimens between 2.2 and 2.7 (see Table 3), which are all relatively low for reinforced concrete members in regions of moderate or high seismic hazard.

5.2.2 Strengthened Columns

Yielding of the three strengthened column specimens (W16-SA, W20-SA, and W25-SA) occurred at a common drift ratio of about $\pm 2.1\%$. Because the splitting cracks were prevented or minimized as a result of the active confinement, neglecting the small difference in the concrete compressive strength, the peak load of the strengthened specimens acquired an increase of about 16.0%, 11.0% and 14.0% when compared with the as-built specimens in test series W16, W20 and W25, respectively. It was apparent from the lateral load-drift response that as a result of suppression of the splitting cracks due to the active confinement as initially anticipated, the spliced bars experienced a predominant pullout mode (as opposed to splitting mode) of bond resistance throughout the response. This behavior enhanced the cyclic bond performance and, in the process, controlled the slip of the starter bars, prevented or minimized pinching of the lateral load-drift response, and reduced significantly the load and stiffness degradations when compared with the as-built specimens. The strengthened specimens were still able to sustain sizable lateral load capacity, even at excessively large drift ratios of $\pm 7.5\%$. The displacement ductility ratios of the three

strengthened columns were all in excess of about 3.4 (See Table 3) which are substantially larger than those developed by the as-built specimens.

5.3 Energy Dissipation Capacities

Figures 30 and 31 show variation of the energy dissipated per one cycle at different cycle numbers for the as-built and strengthened specimens of series W20. The energy was calculated from the area under the lateral load-drift response enclosed within one complete cycle. Cycles 4, 7, 10, 13, 16, 19, 22, and 25 correspond to the first cycle in the target drift ratios of 1, 1.5, 2, 3, 4, 5, 6, and 7.5%, respectively.

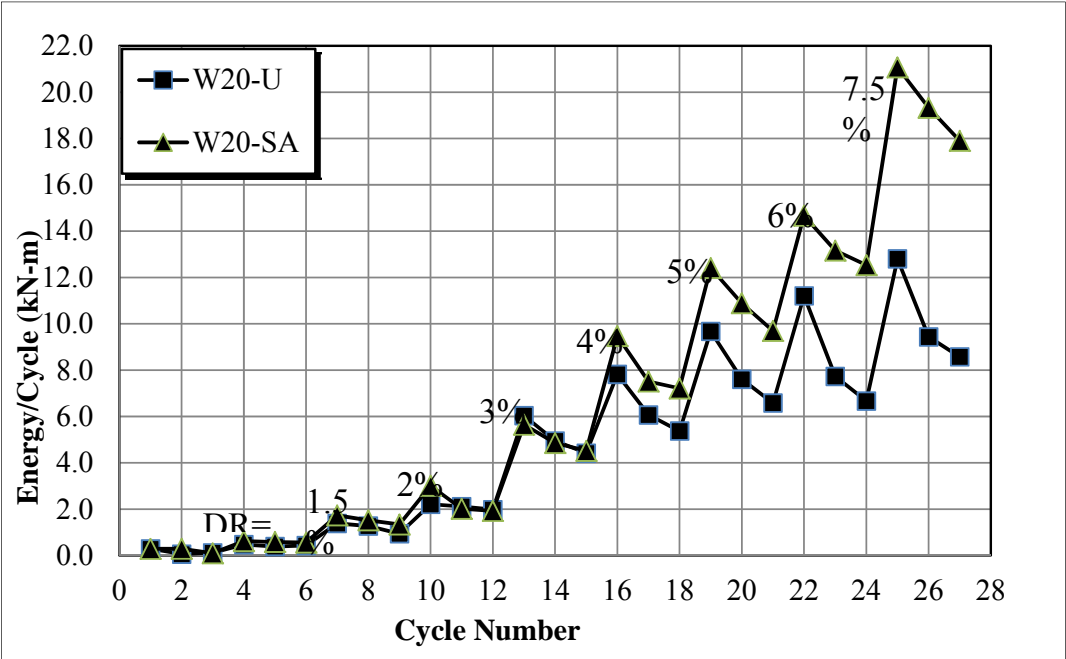


Figure 30. Comparison of energy dissipation of as-built and strengthened specimens of series W20

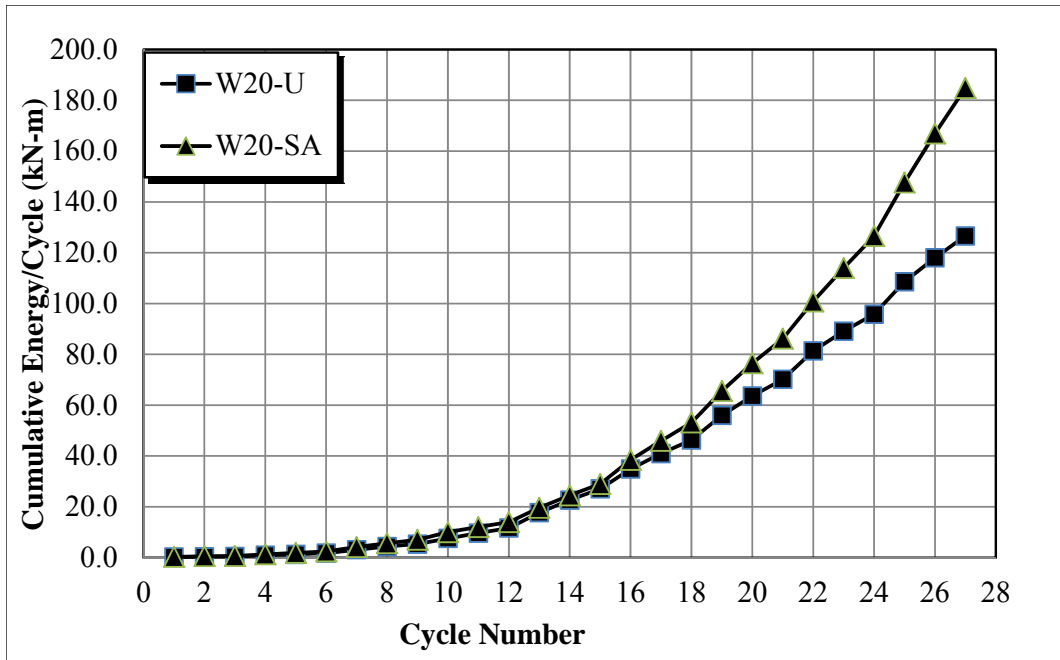


Figure 31. Comparison of cumulative energy dissipation of as-built and strengthened specimens of series W20

At low displacement and up to drift ratios of about $\pm 2.0\%$ to $\pm 3.0\%$, the energy absorption and dissipation capacities of the as-built and the strengthened specimens were almost identical. However, with increase in drift beyond $\pm 3.0\%$ which characterizes regions of high seismic hazard, the energy dissipated by the strengthened columns grew substantially larger, reaching at drift ratios of $\pm 7.5\%$ approximately two times the energy dissipated by their companion as-built columns in test series W20.

CHAPTER 6

CONCLUSIONS

The use of active confinement for seismic bond strengthening of spliced reinforcement in wide rectangular reinforced concrete (RC) columns or wall-type bridge piers is experimentally investigated. Three as-built sample “pier” specimens having lap spliced reinforcement within the critical hinging region were tested under large drift reversals. Companion specimens were strengthened using active confinement by means of pre-tensioning through steel rods and then tested under the same loading protocol as the as-built specimens. The test variables included the ratio of the longitudinal ratio, the bar diameter, and the configuration of the steel anchor rods.

Based on the results of this experimental study, it was found that when subjected to drift reversals induced by even moderate earthquakes, the as-built specimens developed bond splitting cracks which propagated along the full splice length. As a result, these specimens encountered cyclic bond degradation of the spliced reinforcement, leading to inferior performance. Active confinement by means of pre-tensioned steel rods suppressed the development of bond splitting cracks leading to increase in bond resistance of the spliced bars and substantial improvement of seismic performance.

This improved performance is manifested by less concrete damage; lower bond and strength degradation; increase of drift ductility ratios; and lower or insignificant pinching in the lateral load-drift response and consequently enhanced energy dissipation

capacities. Concentrating the active confinement closer to the base of the pier where bond splitting cracks potentially initiate was found to be more effective in improving the bond performance of the lap splices. Nonetheless, more research is needed for identifying the most optimum anchor configuration that would produce the least cost but yet effective seismic strengthening.

Active confinement by means of pre-tensioning steel anchor 1 rods suppressed the development of splitting cracks, altered the bond resistance mechanism from splitting to pullout mode, leading to increase in bond resistance of the spliced bars and substantial improvement of seismic performance of the strengthened columns. This improved performance is manifested by lower bond and strength degradation, increased drift capacity and drift ductility ratios, much lower or insignificant pinching in the lateral load-drift response and considerably enhanced energy dissipation capacities. Concentrating the active confinement closer to the base of the column where splitting cracks potentially initiate was found to be more effective and economical in improving the bond performance of the spliced reinforcement. Nevertheless, more research is needed for identifying the most optimum anchor configuration that would produce the least cost but yet effective seismic strengthening.

A proposed approach is developed for engineers for evaluating the lateral pressure required for adequate bond strengthening and for designing the strengthening system investigated in this study. Also, a design example is provided for illustrating the use of the proposed approach. While the design procedure utilized in this study produced reasonably good strengthening outcomes, the adequacy of the procedure and the effectiveness of the retrofitting technique under investigation require further

experimental verification, particularly for different lap splice lengths and anchor rod pretension force.

REFERENCES

- AASHTO, 1973 “Standard Specifications for Highway Bridges” 11th edition, Washington D.C.
- AASHTO, 2010 “LRFD Bridge Design Specifications” 5th edition, Washington D.C.
- Aboutaha, R. S., Engelhardt, M. D., Jirsa, J. O., and Kreger, M. E., 1999, “Experimental Investigation of Seismic Repair of Lap Splice Failures in Damaged Concrete Columns,” *ACI Structural Journal*, Vol. 96, No. 2, March-April, pp. 297-306.
- ACI Committee 318, 2011, “Building Code Requirements for Reinforced Concrete and Commentary (ACI 318-2011/ACI 318R-11),” American Concrete Institute, Farmington Hills, MI.
- ANSI/AISC 360, 2010, “Load and Resistance Factor Design”, 14th edition, American Institute of Steel Construction, Chicago, IL.
- Aquino, W., and Hawkins, N. M., 2007, “Seismic Retrofitting of Corroded Reinforced Concrete Columns using Carbon Composites,” *ACI Structural Journal*, Vol. 104, No. 3, May, pp. 348-356.
- Darwin, D., Lutz, L.A., and Zuo, J., 2005, ‘Recommended Provisions and Commentary on Development and Lap Splice Lengths for Deformed Reinforcing Bars in Tension’, *ACI Structural Journal*, Vol. 102, No. 6, Nov. Dec., pp. 892-900.
- El Gawady, M., Endeshaw, M., McLean, D., and Sack, R., 2010, “Retrofitting of Rectangular Columns with Deficient Lap Splices” *J. Compos. Construction* 14(1), Jan.-Feb., pp 22-35.
- El Souri, A.M., Harajli M.H., 2011, “Seismic Repair and Strengthening of Lap Splices in RC Columns: Carbon Fiber-Reinforced Polymer versus Steel Confinement,” *ASCE Journal of Composites for Construction*, 15(5), Sept.-Oct., pp. 721-731.
- Eligehausen, R., Popov, E. P., and Bertero, V. V., 1983, “Local Bond Stress-Slip Relationships of Deformed Bars Under Generalized Excitations.” Rep. UCB/EERC-83/23, Uni. of California at Berkeley, Berkeley, Calif.
- Ghosh, K. K., and Sheikh, S. A., 2007, “Seismic Upgrade with Carbon Fiber-Reinforced Polymer of Columns Containing Lap-Spliced Reinforcing Bars,” *ACI Structural Journal*, Vol. 104, No. 2, Mar.-Apr., pp. 227-236.

- Hantouche, E. G., and Harajli, M. H., 2013, "Seismic FRP Bond Strengthening of the Critical Splice Region in Wide Reinforced Concrete Columns," Structures Congress, ASCE, May 2-4, Pittsburgh, PA, USA, pp. 2068-2079.
- Harajli, M. H., 2007, "Numerical Bond Analysis Using Experimentally Derived Local Bond Laws: A Powerful Method for Evaluating the Bond Strength of Steel Bars," Journal of Struct. Engrg., ASCE, 133(5), May, pp. 695-705.
- Harajli, M. H., and Dagher, F., 2008. "Seismic Strengthening of Bond-Critical Regions in Reinforced Concrete Columns Using Fiber-Reinforced Polymer Wraps," ACI Structural Journal, Vol. 105, No. 1, Jan.-Feb., pp. 68-77.
- Harajli, M. H., and Khalil, Z., 2008. "Seismic FRP Retrofit of Bond-Critical Regions in Circular RC Columns: Validation of Proposed Design Methods," ACI Structural Journal, Vol. 105, No. 6, Nov.-Dec., pp. 761-769.
- Harries, K. A., Ricles, J. R., Pessiki, S., and Sause R., 2006, "Seismic Retrofit of Lap Splices in Nonductile Square Columns Using Carbon Fiber-Reinforced Jackets," ACI Structural Journal, Vol. 103, No. 6, Nov.-Dec., pp.874-884.
- Hawkins, N. M., Gamble, W. L., Shkurti, F.J., and Lin, Y., 2000, "Seismic Strengthening of Inadequate Length Splices," 12th World Conference on Earthquake Engineering, Auckland, New Zealand.
- Kim, I., 2008, "Use of CFRP to provide Continuity in Existing Reinforced Concrete Members Subjected to Extreme Loads," PhD dissertation, University of Texas at Austin, TX, 477 pp.
- Kim, I., Jirsa, J. O., and Bayrak, O., 2011, "Use of Carbon Fiber-Reinforced Polymer Anchors to Repair and Strengthen Lap Splices of Reinforced Concrete Columns," ACI Structural Journal, Vol. 105, No. 5, Sept.-Oct., pp. 630-640.
- Mitchell, D., Sexsmith, R., and Tinawi, R., 1994, "Seismic Retrofitting Techniques for Bridges A-State-of-the-Art Report" Journal of Civil Engineering, 21, pp. 823-835.
- Orangun, C.O., Jirsa J.O., and Breen J.E., 1975, "Strength of Anchored Bars: a Reevaluation of Test Data on Development Length and Splices," Research Report No. 154-3F1975, Center for Highway Research, Univ. of Texas at Austin, 78 pp.
- Priestly, M. J. N., and Park, R., 1987, "Strength and Ductility of Concrete Bridges" John Wiley and Sons, New York, NY.

Seible F., Priestly M. J. N., Hegemier G. A., and Innamorato, D., 1997, "Seismic Retrofit of RC Columns with Continuous Carbon Fiber Jackets," *Journal of Comp. for Const., ASCE*, 1(1), pp. 52-62.

Untrauer, R. E., and Henry, R. L., 1965, "Influence of Normal Pressure on Bond Strength," *ACI Journal, Proceedings*, Vol. 62, No. 5, May, pp. 572-585.

Xu, F., Wu, Z, Zheng, J, Hu, Y, and Li, Q., 2014, "Bond Behavior of Plain Bars in Concrete Under Complex Lateral Pressures," *ACI Structural Journal*, Vol. 111, No. 1, Jan.-Feb., pp. 15-25.

